

## Nanoscale domains with nematic order in supercooled vitamin-A acetate: Molecular dynamics studies

Z. Wojnarowska,\* M. Paluch, P. Włodarczyk, L. Hawelek, R. Wrzalik, and J. Ziolo  
*Institute of Physics, University of Silesia, ul. Uniwersytecka 4, PL-40-007 Katowice, Poland*

M. Wygledowska-Kania, B. Bergler-Czop, and L. Brzezinska-Wcislo  
*Department of Dermatology, Silesian Medical University in Katowice, Francuska Street 20/24, PL-40-027 Katowice, Poland*

P. Bujak

*Institute of Chemistry, Faculty of Mathematics, Physics and Chemistry, University of Silesia ul. Szkolna 9, PL-40-007 Katowice, Poland*

(Received 20 December 2010; published 9 May 2011)

Vitamin-A acetate is one of the most versatile vitamins. It is applied in medicine because of its antioxidative properties, in tumor therapy because of its cytostatic activity, and in cosmetics because of its nutritional additives. Herein, using broadband dielectric spectroscopy, the molecular dynamics of supercooled and glassy vitamin-A acetate was investigated. It was shown that dielectric measurements carried out at ambient and elevated pressures reveal a number of relaxation processes associated with different types of molecular motions:  $\alpha$ ,  $\delta$ , and  $\nu$  processes—observed above the glass transition temperature and the next two modes:  $\beta$  and  $\gamma$  identified in the glassy state. The occurrence of the  $\delta$  mode in the dielectric spectrum may imply the existence of nanoscale domains with nematic order. This hypothesis is further checked by atomic force microscopy measurements. Finally, we have determined the value of the glass transition temperature ( $T_g$ ) as well as the steepness index ( $m_p$ ) at various  $T$ - $P$  conditions.

DOI: [10.1103/PhysRevE.83.051502](https://doi.org/10.1103/PhysRevE.83.051502)

PACS number(s): 64.70.pp, 77.22.Gm

### I. INTRODUCTION

Relaxation dynamics of glass-forming liquids has been extensively investigated not only for the purpose of deeper understanding of the vitrification process of liquids, but also for practical application reasons [1–5]. For conventional glass-forming liquids, the two-step relaxation scenario is commonly observed in the vicinity of glass transition temperature  $T_g$ . It means that two relaxation modes occur in the relaxation spectrum obtained by various spectroscopic methods including broadband dielectric spectroscopy (BDS), nuclear magnetic resonance (NMR), or mechanical spectroscopy. The slower  $\alpha$ -relaxation mode arises from molecular structure rearrangements, and it is directly related to the liquid-glass transition. These molecular rearrangements have cooperative character, and the number of molecules involved in the motion is believed to grow when approaching the glass transition temperature [6,7]. On the other hand, a more localized type of motion is assumed to be responsible for a second (faster) relaxation mode, usually denoted as a  $\beta$  process. In fact, two classes of the secondary ( $\beta$ ) process can be distinguished due to the different molecular mechanisms. While one class is related to the trivial rotational motion of small isolated groups of molecules or conformational changes, the second one includes processes that effectively involve the motion of the entire molecule. In the last case, molecular motion is completely determined by intermolecular interactions, and, therefore, such a relaxation process has a connection to the cooperative  $\alpha$ -relaxation process [8,9].

As already mentioned, the molecular dynamics has also been studied in the context of practical applications. In the

past several years, considerable attention has been focused on the formulation of drugs in an amorphous state as a way for enhancing the bioavailability of poorly soluble pharmaceutical compounds [10–12]. However, a serious problem that is encountered is that amorphous pharmaceuticals often undergo unwanted physical and chemical transformations during processing and storage [13,14]. It results from the fact that the molecular mobility of the amorphous form is higher than its crystalline counterpart. Therefore, the complete characterization of molecular dynamics of amorphous pharmaceutical compounds under various thermodynamic conditions is currently of paramount importance for designing and producing amorphous drugs with a desired stability.

One of the important and interesting aspects of molecular dynamics studies is finding a connection between molecular relaxation pattern of glass-forming liquids and shape and structure of molecules. It has to be realized that the shape of molecules determines the character of intermolecular interactions that are responsible for their dynamic properties. Recently, the effect of shape and size of hard ellipsoids on their glassy behavior was theoretically studied in Ref. [15] by the application of the ideal mode-coupling theory. The results presented by the authors of Ref. [15] imply that, in the case of liquids consisting of rigid rodlike molecules, the liquid-glass transition should be primarily driven by an orientational degree of freedom. Consequently, it is expected that nanoscale domains with nematic order can be formed when approaching the glass transition. However, these predictions require experimental testing. Overall, it is highly desired to check experimentally whether there is any difference in the relaxation behavior between the rodlike system and the conventional glass-forming liquids exhibiting two-step relaxation dynamics. In this respect, we have experimentally investigated the

\*zwojnaro@us.edu.pl

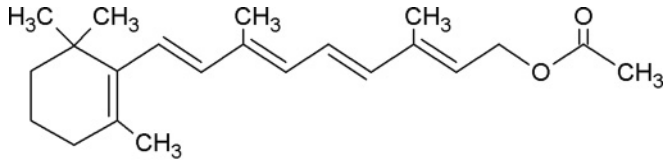


FIG. 1. Chemical structure of all-*trans* vitamin-A acetate.

molecular dynamics of supercooled vitamin-A acetate, whose molecules have a nearly rodlike shape. Vitamin-A acetate is one of many forms of vitamin A, and it is commonly used in antiaging chemicals [16]. The molecular dynamics was monitored as a function of both temperature and pressure using BDS. These studies were supplemented by atomic force microscopy (AFM) measurements of surface topography and by density functional theory (DFT) calculations. In addition, we performed x-ray diffraction (XRD) and NMR measurements to confirm amorphous and chemical structures of the vitrified sample.

## II. EXPERIMENTAL AND CALCULATION METHODS

### A. Material

The crystalline form of vitamin-A acetate (also called retinyl acetate) of 97% purity and molecular mass of  $M_w = 328.49$  g/mol was supplied as a yellow powder from Sigma-Aldrich, and it was used without any further purification. The starting material was completely crystalline with the melting point equal to 331 K. The NMR measurements have shown that the retinyl sample does not undergo any chemical decomposition at the melting temperature. However, it is worth mentioning that both naturally occurring vitamin A and its synthetic counterparts often coexist with their *cis-trans* isomers. The NMR measurements confirmed that the examined sample is all-*trans*-3,7-dimethyl-9-(2,6,6-trimethyl-1-cyclohexene-1-yl)-2,4,6,8-nonatetraene-1-ylacetate with the structure presented in Fig. 1.

### B. BDS

Isobaric measurements of the dielectric permittivity  $\varepsilon^*(\omega) = \varepsilon'(\omega) - i\varepsilon''(\omega)$  at ambient pressure in a wide temperature range (139–299 K) were carried out using the Novocontrol  $\alpha$  dielectric spectrometer over the frequency range from  $10^{-2}$  to  $10^7$  Hz. Dielectric measurements of supercooled vitamin-A acetate were performed after melting of the crystalline material in a parallel-plate cell of a capacitor (diameter: 20 mm, gap: 0.1 mm). The temperature was controlled by Quatro System using a nitrogen gas cryostat. The temperature stability was better than 0.1 K.

For the pressure dependent dielectric measurements, we used a capacitor, filled with the retinyl acetate sample, which next was placed in the high-pressure chamber and was compressed using the silicone fluid via a piston in contact with a hydraulic press. The sample was in contact only with stainless steel and teflon. Pressure was measured by the Nova Swiss tensometric pressure meter with a resolution of 0.1 MPa. The temperature was controlled within 0.1 K by means of a liquid flow provided by a thermostatic bath.

### C. NMR Spectroscopy Measurements

The 400-MHz  $^1\text{H}$  NMR spectra were recorded on a Bruker Avance 400 spectrometer at 298 K for 5-wt % solutions in dimethyl sulfoxide (DMSO)- $d_6$ . The chemical shifts are expressed on the  $\delta$  scale relative to internal TMS.

The crystalline sample of retinyl acetate.  $^1\text{H}$  NMR (400 MHz, DMSO- $d_6$ )  $\delta = 1003$  ppm (s, 6H,  $2 \times \text{CH}_3$ ); 1418–1447 [m, 2H,  $\text{CH}_2-\text{C}(\text{CH}_3)_2$ ]; 1539–1599 [m, 2H,  $\text{CH}_2-\text{CH}_2-\text{C}(\text{CH}_3)_2$ ]; 1674 (s, 3H,  $\text{CH}_3\text{C} = \text{C}$ ); 1849 (s, 3H,  $\text{CH}_3-\text{C} = \text{CH}-\text{CH}_2\text{O}$ ); 1926 [s, 3H,  $\text{CH} = \text{CH}-\text{C}(\text{CH}_3)-\text{CH}$ ]; 1993 [t, 2H,  $\text{CH}_2-\text{C}(\text{CH}_3) = \text{C}$ ,  $J = 6,10$  Hz]; 2010 (s, 3H,  $\text{CH}_3-\text{CO}$ ); 4677 (d, 2H,  $\text{CH}_2\text{O}$ ,  $J = 7,20$  Hz); 5611 (t, 1H,  $= \text{CH}-\text{CH}_2\text{O}$ ,  $J = 7,20$  Hz); 6111 (d, 1H,  $= \text{C}-\text{CH} = \text{CH}$ ,  $J = 16,1$  Hz); 6149 (d, 1H,  $\text{C} = \text{CH}-\text{CH} = \text{CH}$ ,  $J = 11,10$  Hz); 6166 (d, 1H,  $= \text{C}-\text{CH} = \text{CH}$ ,  $J = 16,1$  Hz); 6325 (d, 1H,  $\text{C} = \text{CH}-\text{CH} = \text{CH}$ ,  $J = 15,00$  Hz); 6658 (dd, 1H,  $\text{C} = \text{CH}-\text{CH} = \text{CH}$ ,  $J = 15,00$  Hz,  $J = 11,10$  Hz).

### D. AFM

The AFM visualization of the vitamin-A acetate sample surface in three dimensions was performed using the NT-MDT Solver P47-PRO microscope. The measurement was made in the tapping mode to minimize the interaction of a tip on the sample surface. The rectangular silicon cantilever with a trapezoidal cross section was used (nanosensors probe; a nominal elastic constant of 7.4 N/m and a nominal resonance frequency 160 kHz). Scanning speed during the acquisitions ranged from 300 to 500 nm/s. The tip oscillation amplitude was about 25 nm. During the scanning, the topography (height) and the vibrating phase images were recorded in the same time. The retinyl sample for the AFM measurement was prepared by the same temperature treatment like the dielectric one—0.5 mg of crystalline retinyl was placed on a glass microscope plate and was heated to the temperature 333 K in air and was quickly cooled to the room temperature. The surface of the glass-formed retinyl drop was under AFM investigation. All measurements were performed at room temperature.

### E. XRD measurements

XRD measurements of the structure of crystalline and amorphous vitamin-A acetate were carried out at room temperature ( $T = 293$  K) on the laboratory Rigaku-Denki D/MAX RAPID II-R diffractometer attached to a rotating anode Ag  $K\alpha$  tube ( $\lambda = 0.5608$  Å), an incident beam (0 0 2) graphite monochromator, and an image plate in the Debye-Scherrer geometry. The pixel size was  $100 \times 100$   $\mu\text{m}$ . Samples of vitamin-A acetate were placed inside glass capillaries (1.5 mm in diameter). Measurements were performed for the filled sample and empty capillaries, and the intensity for the empty capillary was then subtracted. The beam width at the sample was 0.1 mm. The two-dimensional diffraction patterns were converted into the one-dimensional intensity data using suitable software.

### F. Calculation methods

The vitamin-A acetate molecule has been optimized at the B3LYP/6-31+ $g^*$  level. The presented structure is in the minimum due to the position of the acetyl group, which

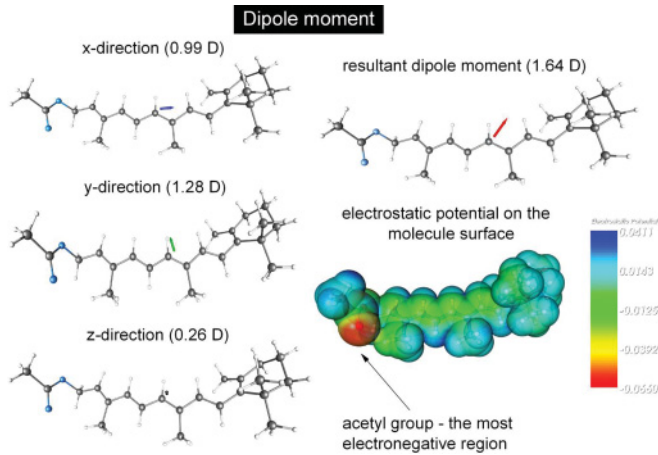


FIG. 2. (Color online) Components of the dipole moment (in the  $x$ ,  $y$ ,  $z$  directions) as well as the resultant dipole moment were drawn.  $x$ -direction component of the dipole moment has a similar magnitude to the  $y$ -direction component. The oxygen atom from the acetyl group has the most negative electrostatic potential, thus, rotation of the acetyl group should be connected to the significant dipole moment fluctuations.

is the most flexible part of the molecule. It was found by numerous optimizations of different conformations due to the acetyl group placement. The relaxed geometry scan by changing the proper dihedral angle was performed in order to simulate rotation at the B3LYP/6-31+g\* level of theory. Thereafter, the structure characterized by the highest value of electronic energy was optimized as a transition state by means of an eigenvector following method. Transition state and minima were further confirmed by performing vibrational analysis. Frequencies were calculated numerically at the same level of theory. All these calculations were performed with the ORCA quantum package [17]. Moreover, electrostatic potential was calculated by means of the GAUSSIAN 03 program package [18]. Molecules were visualized by means of the GOPENMOL and MOLEKEL packages. Ellipsoid parameters were found by performing intramolecular distance measurements in GOPENMOL.

### III. RESULT AND DISCUSSION

The chemical structure of vitamin-A acetate is depicted in Fig. 1. It can be noted that a sequence of four double bonds in the alkyl chain represents a very stiff part of the retinyl molecule. Therefore, one can expect that the molecule has an elongated rodlike shape. This supposition was confirmed by calculations within the framework of DFT performed on a single molecule in vacuum. As can be seen in Fig. 2, the vitamin-A acetate molecule optimized at the B3LYP/6-31+g\* level has a slight banana shape. However, it can also be approximated satisfactorily by an ellipsoid. The semimajor axis ( $a$ ) of such an ellipsoid is equal to approximately 9.0 Å, while semiminor axes ( $b$ ) and ( $c$ ) are equal to 4.0 and 4.3 Å, respectively. Therefore, the proportion of the semimajor axis to the longer semiminor axis is equal to 2.1, and the molecule is strongly anisotropic. In Fig. 2, one can observe the dipole moment analysis in the retinyl acetate. The three components

of the dipole moment vector are presented in this figure. The magnitude of the  $x$  component (0.99 D), which is parallel to the semimajor axis of the molecule, is comparable to the magnitude of the  $y$  component (1.28 D), which is perpendicular to the semimajor axis and is parallel to the one of semiminor axes of the molecule. The dipole moment of the entire molecule mainly depends on the orientation of the terminal acetyl group, which is clearly seen on the electrostatic potential plot. However, the placement of electronegative oxygen in the acetyl group determines the magnitude and direction of the resultant dipole moment vector.

#### A. Molecular mechanisms above and below $T_g$ at ambient pressure

The vitamin-A acetate sample was studied both above and below the liquid-glass transition. In order to confirm the amorphous nature of the tested material, the XRD technique was applied. Since we have found that the amorphous vitamin-A acetate reveals the crystallization tendency, the X-ray measurements were additionally performed on the same sample that was previously measured by dielectric spectroscopy. In all cases, the diffraction patterns were characteristic for the amorphous state.

To investigate the orientational dynamics of vitamin-A acetate molecules both in the supercooled regime and in the glassy state, we measured dielectric spectra in the frequency range from  $10^{-2}$  to  $10^7$  Hz. The frequency behavior of the dielectric permittivity losses  $\varepsilon''(\omega)$  for the sample at various temperatures above the glass transition temperature is shown in panel (a) of Fig. 3. As can be seen, the relaxation spectra are much more complicated than would be obtained for the typical glass-forming liquids. For this material, we observe a number of relaxation processes associated with different types of molecular motions. As usual, the dc conductivity contributes to the dielectric loss response at the lowest frequency. This part of the dielectric spectrum can be described by the power law,

$$\varepsilon(\omega)'' = \frac{\sigma_{dc}}{\varepsilon_0 \omega}, \quad (1)$$

where  $\sigma_{dc}$  and  $\varepsilon_0$  are the dc electrical conductivity and permittivity of free space, respectively. The dc-conductivity contribution occurs due to a small concentration of mobile impurity ions. However, the characteristic feature of orientational dynamics of supercooled retinyl acetate is the presence of a very broad relaxation peak, which nearly spans the entire frequency window. A closer inspection of the shape reveals the occurrence of three relaxation processes, labeled with Greek letters:  $\nu$ ,  $\delta$ , and  $\alpha$ . To analyze the dielectric spectra quantitatively, the data in Fig. 3(a) were fitted using the superposition of three Havriliak-Negami (HN) functions with the dc-conductivity term added [Eq. (2)] [19],

$$\varepsilon(\omega)'' = \frac{\sigma_{dc}}{\varepsilon_0 \omega} + \text{Im} \sum_{i=1}^3 \left( \varepsilon_{\infty} + \frac{\Delta \varepsilon_i}{[1 + (i\omega \tau_i)^{\alpha_i}]^{\beta_i}} \right), \quad (2)$$

where  $\alpha$  and  $\beta$  are the shape parameters that characterize the symmetric and asymmetric broadenings of a given relaxation peak,  $\Delta \varepsilon$  is the dielectric relaxation strength, and  $\tau$  denotes the relaxation time. Figure 3(b) shows a representative fit of the experimental data measured at  $T = 273$  K. As can be seen

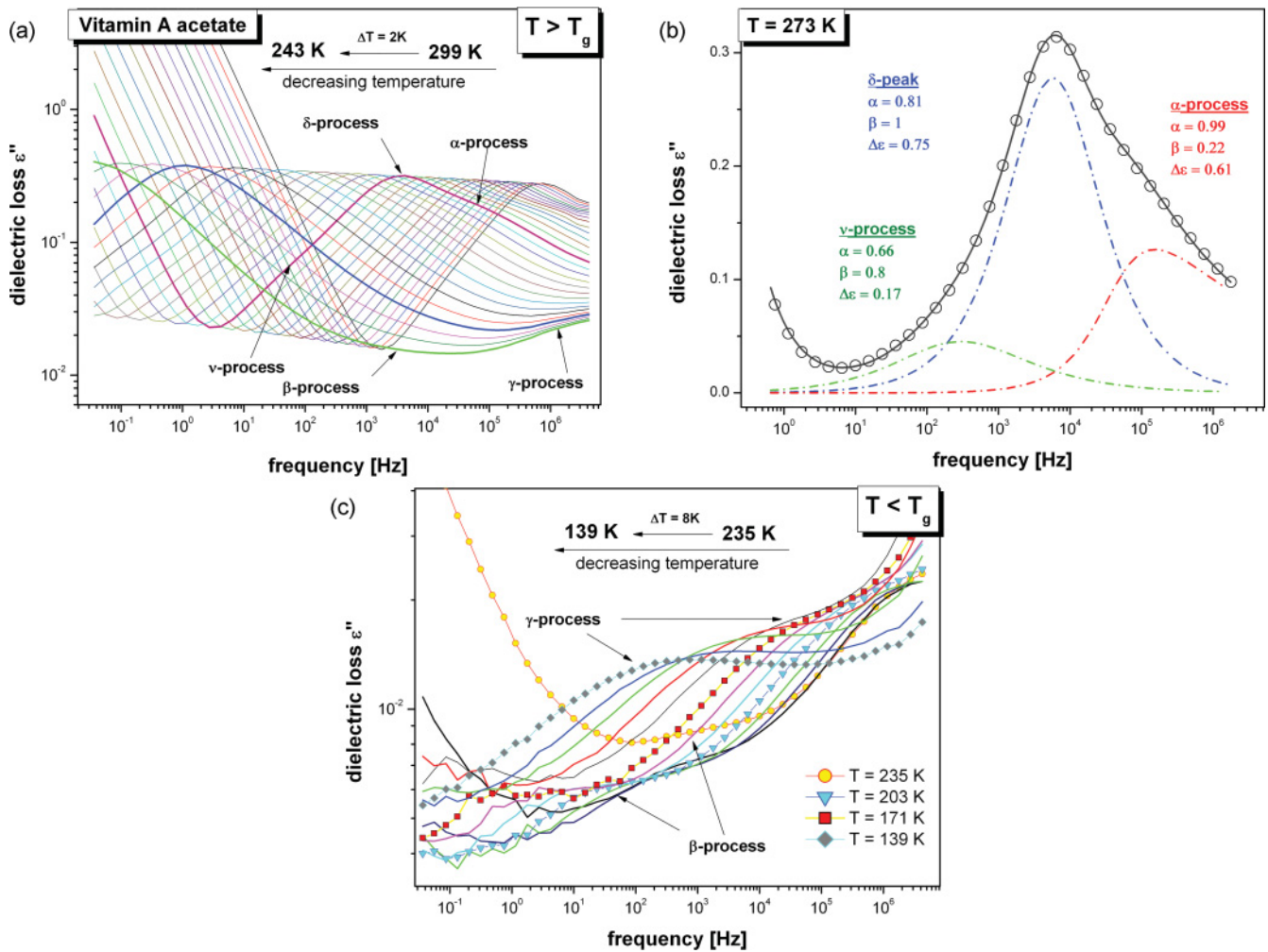


FIG. 3. (Color online) Dielectric loss spectra of vitamin-A acetate obtained at ambient pressure. Panel (a) presents dielectric loss above the glass transition temperature. In panel (b), the example of the fitting procedure of the selected dielectric loss spectrum obtained in the liquid state of vitamin-A acetate ( $T = 273$  K) is depicted. Solid lines depict the fit of the entire spectrum based on the superposition of three HN functions. In panel (c), dielectric loss spectra below  $T_g$  are presented.

in this plot, the most pronounced relaxation peak, denoted by  $\delta$ , has a symmetric shape. This relaxation is only slightly broader than the simple Debye function. On the other hand, at high frequencies, there is a much broader asymmetrical  $\alpha$  peak probably due to the cooperative motions of the retinyl acetate molecules. Thus, the  $\alpha$ -relaxation process is considered to be responsible for the relaxation of the molecular structure, the viscous flow, and the liquid-glass transition. There is also the third  $\nu$ -relaxation peak, which is localized in close proximity of the  $\delta$  process at the low-frequency range.

Discussing the origin of the  $\delta$ -relaxation process, it might be useful to recall the dielectric studies of the glass-forming mixture of liquid crystals (E7) [20,21]. As in the case of vitamin A, three similar relaxation modes were also distinguished in the supercooled nematic phase of E7. It was shown that the most prominent (Debye-like) relaxation process has its origin in the  $180^\circ$  rotation of the molecules around their molecular short axes. On the other hand, the peak occurring at the high-frequency flank was assigned as the  $\alpha$ -process. Interestingly, the same pattern of behavior, as in the case of E7, is also observed for vitamin A, i.e., the two processes,  $\alpha$  and  $\delta$ ,

collapse into one broadened relaxation as the glass transition temperature is achieved. Taking all mentioned similarities into account, it is reasonable to propose that the symmetric and narrow  $\delta$ -mode, visible in the relaxation spectra of retinyl acetate, arises from rotational fluctuations of the molecule around the short axis. Additionally, the occurrence of the  $\delta$ -mode in the dielectric spectrum of vitamin-A acetate may imply the existence of nanoscale domains with nematic order as theoretically predicted in Ref. [15].

Finally, we can try to explain the origin of the small  $\nu$ -relaxation peak localized at the low-frequency range, based on the assumption of the existence of nanoscale domains with nematic domains. The investigated material became heterogeneous on account of the occurrence of nanoscale domains with nematic order. The polarization on the domains boundary leads to the charge's accumulation on the interfaces where materials of different electrical properties contact each other [22]. Due to the heterogeneity of the investigated material, one can suppose that the third process, visible in the dielectric spectrum of vitamin A, may be attributed to the Maxwell-Wagner effect. As can be seen in Figs. 3 and 10, the

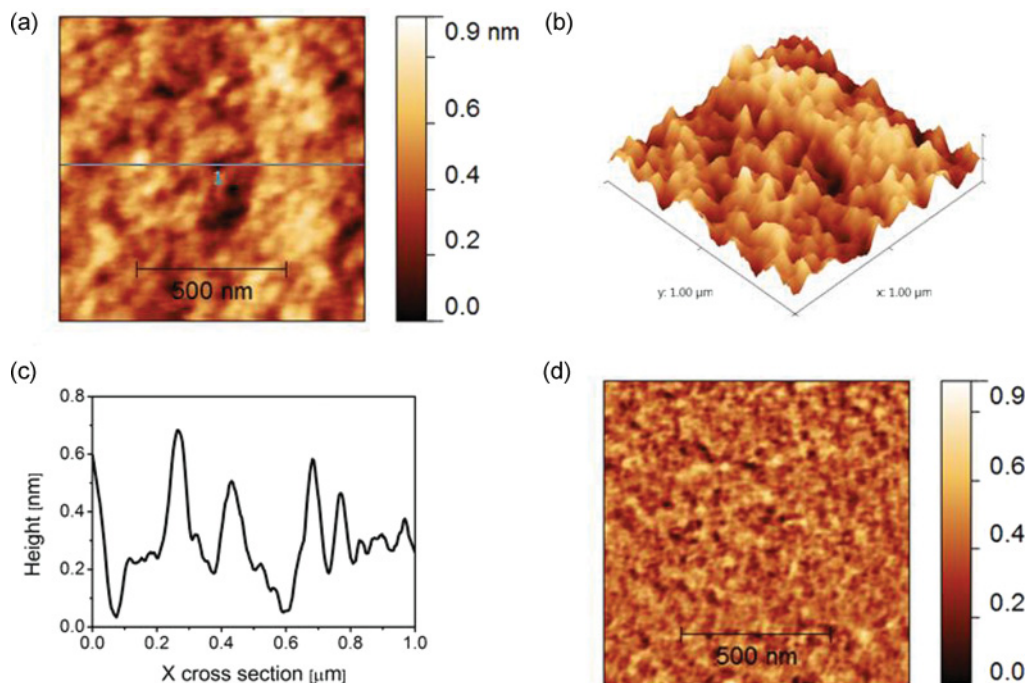


FIG. 4. (Color online) AFM images of the retinyl drop surface: (a) topography, (b) topography three-dimensional view, (c) selected cross sectional profile, and (d) phase; (images scale  $1 \times 1 \mu\text{m}$ ).

amplitude of the  $\nu$  process is changing with temperature and pressure. The observed effect is probably related to the changes of the domain's size, which are growing at lower temperatures and higher pressures.

In order to confirm the existence of the nanoscale domains, the AFM visualization of the retinyl acetate sample surface was performed. In Fig. 4, the topography and phase contrast mode images are presented. Both pictures show the adjacent grain of the size 50–200 nm. The analysis of topography cross sections shows that the amount of these grains ranges from 100 to 300 nm. It can be assumed that grains are formed as areas of local ordering of molecules. Local order in the area of a single grain cannot be observed, unfortunately, due to the resolution of the microscope (measurements were made in air). The occurrence of a tendency for the parallel arrangement of vitamin-A molecules is not obvious, but as a survey of  $n$  alkanes, even soft long-chain molecules tend to organize in the nematic order [23]. The existence of microscopic domains is also shown in a Fig. 4(c) phase shift of an oscillating microscope tip. However, in this case, the picture is more complicated, since the phase change results from the elastic properties of the material (difference in viscoelasticity of the domains and the borders between them) as well as the capillary effects—in the air, the surface is covered with a layer of water.

The dielectric spectra collected at temperatures lower than the glass transition temperature are presented in Fig. 3(c). In the glassy state, two secondary relaxation processes  $\beta$  and  $\gamma$  can be identified. They can be well described by the Cole-Cole function. The  $\beta$ -relaxation originates from local fluctuations of the entire molecule, whereas, internal mobility of the molecule may lead to a rising faster secondary  $\gamma$ -process. The details of

the molecular motions responsible for the  $\gamma$ -relaxation will be presented in a later part of this paper.

The temperature dependences of relaxation times  $\tau_\delta$ ,  $\tau_\alpha$ ,  $\tau_\beta$ , and  $\tau_\gamma$ , are shown in the Arrhenius plot depicted in Fig. 5. All relaxation times were determined as the inverse of the frequency in the maximum of loss peak ( $\tau = 1/2\pi f_{\text{max}}$ ). As suggested by the results presented in Fig. 5, the two curves  $\log \tau_\alpha(1/T)$  and  $\log \tau_\delta(1/T)$  merge approaching the glass transition. Therefore, only one broad relaxation peak is observed in the vicinity of  $T_g$  [see Fig. 3(a)]. In the case

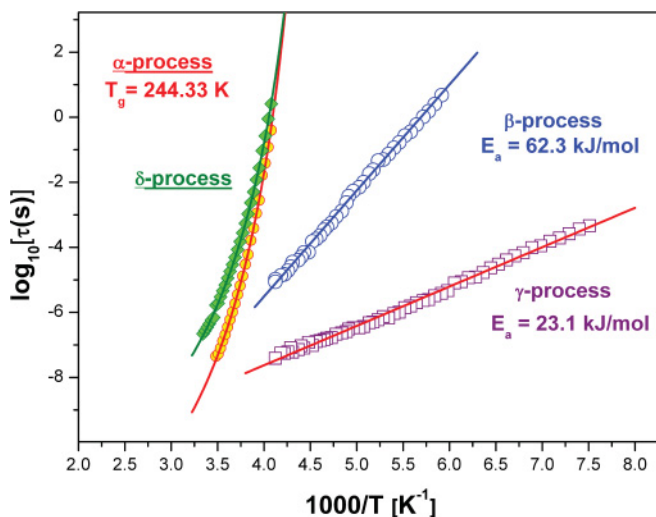


FIG. 5. (Color online) The relaxation map of vitamin-A acetate.  $\tau_\alpha(T^{-1})$  and  $\tau_\delta(T^{-1})$  are depicted as solid yellow circles and solid green squares, respectively, while the  $\beta$ - and  $\gamma$ - relaxation times are visible as open blue circles and open violet squares, respectively.

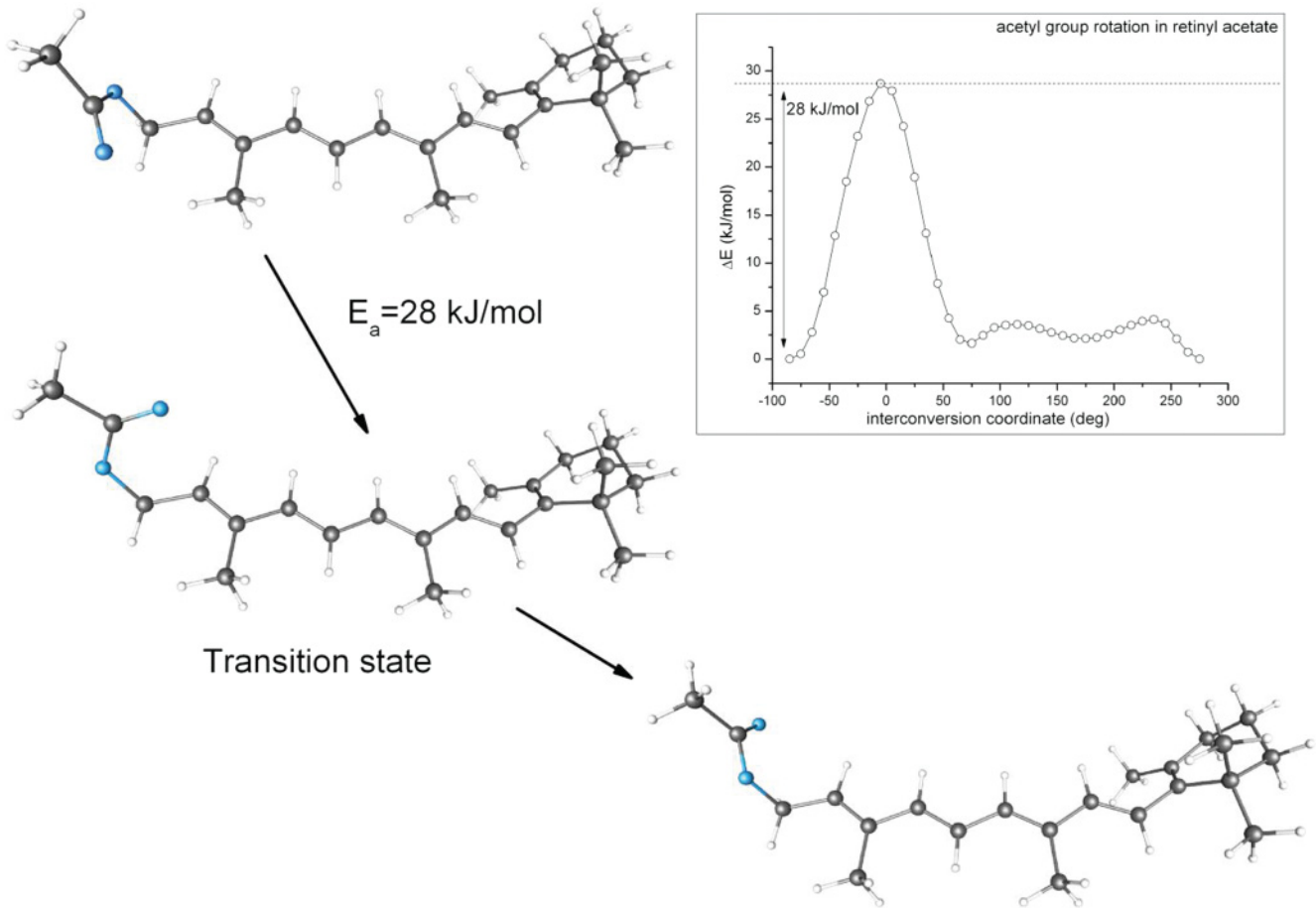


FIG. 6. (Color online) Visualization of conformational interconversion connected to the acetyl group rotation. In the inset, there is a diagram, which represents changes of energy during the rotation.

of both mentioned dependences, the usual non-Arrhenius behavior was found. Therefore, these experimental data can be fairly well described by means of the Vogel-Fulcher-Tammann (VFT) equation [24–26],

$$\tau_{\alpha} = \tau_0 \exp\left(\frac{DT_0}{T - T_0}\right), \quad (3)$$

with the following fitting parameters: for the  $\alpha$ -process  $\log \tau_0 = -15.21 \pm 0.34$ ,  $D = 3.4 \pm 0.25$ ,  $T_0 = 199.7 \pm 1.9$  K; for the  $\delta$ -process  $\log \tau_0 = -12.94 \pm 0.23$ ,  $D = 3.17 \pm 0.18$ ,  $T_0 = 198.1 \pm 1.6$  K.

From  $\tau_{\alpha}(T)$  dependence, we have determined the glass transition temperature of vitamin-A acetate. To avoid the extrapolation of VFT fits in our analysis, we have defined  $T_g$  as a temperature at which  $\tau_{\alpha} = 1$  s. Its value at ambient pressure conditions is equal to 244.33 K.

Now, we focus on the analysis of the secondary relaxation process detected in the dielectric loss spectra of vitamin-A acetate. As can be seen in Fig. 5, the relaxation times of both secondary relaxation processes show the Arrhenius behavior below  $T_g$ . The values of activation energy for both  $\beta$ - and  $\gamma$ -modes, obtained from fitting the Arrhenius law to the experimental data, are equal to 62 and 23 kJ/mol, respectively. The low value of activation energy for  $\gamma$ -relaxation implies that the intramolecular motions might be involved. Indeed, this

expectation has been strongly confirmed by DFT calculations. It is well known that the secondary mode can be observed by means of BDS if the dipole moment is changing during conversion [27]. Therefore, we have studied conformational interconversion, which is connected to the acetyl group rotation. As mentioned in the previous part of this paper, the acetyl group is strongly electronegative. Therefore, during its reorientation, the value of the dipole moment of the molecule is changing significantly. In Fig. 6, one can see the route of the acetyl group rotation. The value of the activation energy of such a movement obtained in the B3LYP/6-31+g\* model is equal to 28 kJ/mol, and it corresponds to the activation energy of the  $\gamma$  mode determined experimentally.

### B. Effects observed at elevated pressure

Isothermal measurements were performed at  $T = 283$  K by varying pressure from 80 to 240 MPa. Unfortunately, we were not able to measure the dielectric spectra below 80 MPa because the examined sample had quite a strong tendency for recrystallization. It is well known that compression basically has the same effect on the dielectric loss spectra behavior as lowering the temperature. That is why the relaxation peaks of vitamin-A acetate move toward lower frequencies with elevating pressure (see Fig. 7). As can be seen in Fig. 7, the tendency to merge  $\delta$ - and  $\alpha$ -relaxation modes into a broad one

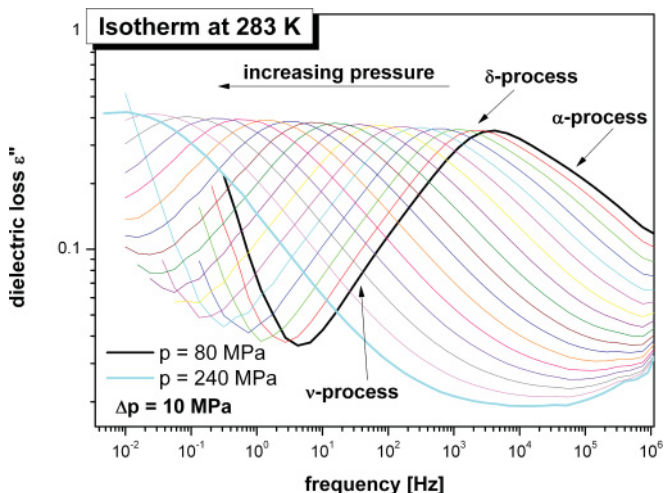


FIG. 7. (Color online) Loss spectra obtained during isothermal measurement carried out at  $T=283$  K ( $p=80-240$  MPa).

is again observed when the liquid-glass transition is achieved by squeezing the liquid sample. To determine the  $\delta$ - and  $\alpha$ -relaxation times, the same fitting procedure as previously described was used. As depicted in Fig. 8, both relaxation times approximately increase with pressure in the linear fashion. Thus, to parametrize these two dependences, one can apply the simple Arrhenius law written in the following form [28,29]:

$$\log \tau = \log \tau_0 + \frac{P \Delta V}{RT} \log e. \quad (4)$$

The values of activation volume determined from the fitting analysis are equal to  $180 \pm 2$  and  $189 \pm 2$   $\text{cm}^3/\text{mol}$  for the  $\delta$ - and  $\alpha$ -relaxation processes, respectively. According to the transition state theory, the activation volume defines the additional space, which has to be created to move the relaxing molecules to another position [30]. Thus,  $\Delta V$

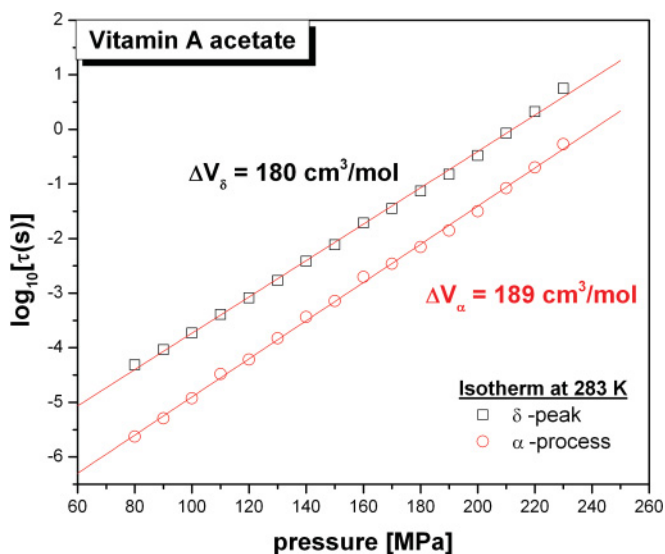


FIG. 8. (Color online) The pressure dependences of the relaxation times  $\tau_\alpha$  and  $\tau_\delta$  at constant temperature ( $T=283$  K). Straight lines are fits using Eq. (4).

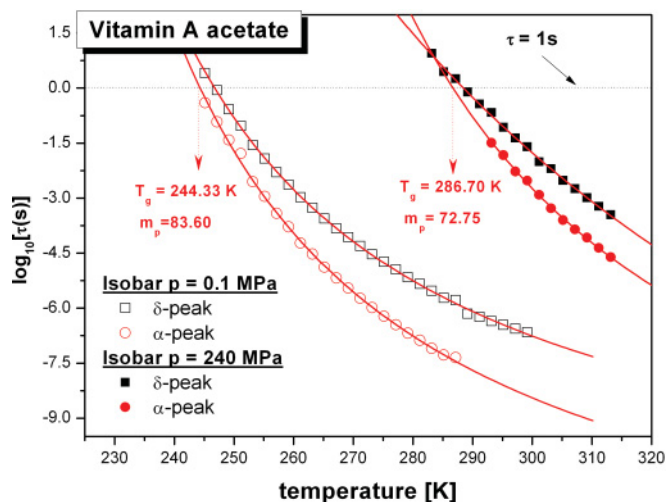


FIG. 9. (Color online) Structural relaxation times  $\tau_\alpha$  and  $\tau_\delta$  obtained during isobaric measurements. Solid lines are VFT fits for the experimental data.

reflects the volume requirements for local molecular motions. Considering that molecules involved in the  $\alpha$ -relaxation process move cooperatively, one can expect that the value of the activation volume for this process should be slightly larger than for the noncooperative  $\delta$ -relaxation. This expectation is indeed in agreement with our experimental result, i.e.,  $\Delta V_\alpha > \Delta V_\delta$ .

An important aspect of the analysis of the molecular dynamics is the behavior of temperature dependence of the structural relaxation times at elevated pressure. In this connection, we have also performed the dielectric measurements at  $p=240$  MPa. From the collection of data obtained isobarically at 240 MPa as a function of temperature, the  $\alpha$ - and  $\delta$ -relaxation times have also been determined and have been plotted as a function of temperature in Fig. 9. As can be seen similarly as in the case of the data collected at ambient pressure, one can observe the non-Arrhenius behavior of  $\log \tau_\alpha(T)$  and  $\log \tau_\delta(T)$  that can be satisfactorily described with the use of the VFT equation. Unfortunately, even if the glass transition temperature is defined as the temperature at which  $\tau_\alpha$  reaches 1 s, to determine the value of  $T_g$  at high pressure, the extrapolation of measurement for the longer times is necessary. It is because, with decreasing temperature, both relaxation processes  $\alpha$  and  $\delta$  are getting closer, and it is hard to determine the maximum of the  $\alpha$ -loss peak near the liquid-glass transition. Based on the VFT fits, the  $T_g$  of vitamin-A acetate at 240 MPa was determined and was illustrated in Fig. 9. It is clearly seen that the experimentally determined glass transition temperature of vitamin-A acetate is strongly dependent on pressure. The value of  $T_g$  is changing almost 17% with increasing pressure from 0.1 to 240 MPa. Therefore, one can expect the large value of the pressure coefficient of the glass transition temperature. In the limit of low pressures, it is equal to 235 K/GPa. This value is similar to that obtained for the van der Waals materials (200–300 K/GPa) and significantly larger than values achieved for typical H-bonding systems, such as glycerol (40 K/GPa) [31] or sorbitol (43 K/GPa) [32]. Also, it is worth mentioning that

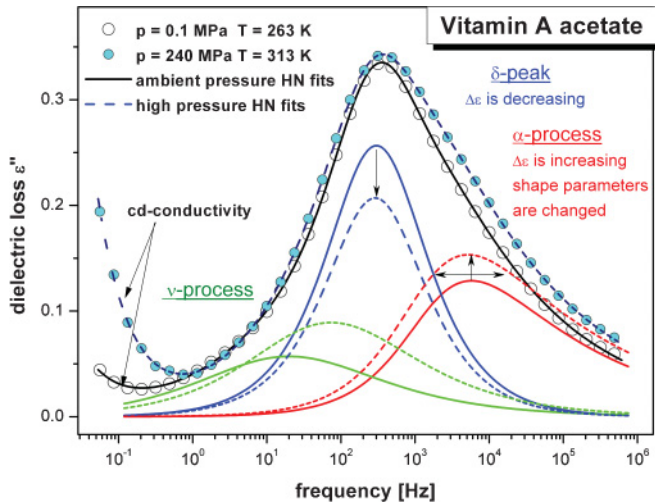


FIG. 10. (Color online) The comparison of the shape of the dielectric loss spectra characterized with the same  $\tau_\delta$  but obtained at different  $T, P$  conditions. The solid line depicts the HN fit of the spectrum collected at ambient pressure, whereas, the dashed line indicates the HN fit of the high-pressure data. The fitting parameters of the data, collected at elevated pressures, are equal to:  $\delta$ -peak,  $\alpha = 0.81$ ,  $\beta = 1$ , and  $\Delta\epsilon = 0.57$ ;  $\alpha$ -peak,  $\alpha = 0.78$ ,  $\beta = 0.31$ , and  $\Delta\epsilon = 0.76$ ;  $\nu$ -peak,  $\alpha = 0.56$ ,  $\beta = 0.8$ , and  $\Delta\epsilon = 0.4$ . The HN-fitting parameters of the data collected at ambient pressure conditions are presented in Fig. 3.

the isobaric fragility ( $m_P$ ) calculated on the basis of VFT fits [33],

$$m \equiv \left. \frac{d \log \tau_\alpha}{d(T_g/T)} \right|_{T=T_g} \quad (5)$$

follows the same pattern of behavior as established experimentally for van der Waals liquids—it decreases with increasing pressure [34–36]. Its value is decreasing from  $m_P = 83$  at ambient pressure to  $m_P = 72$  at 240 MPa. It means that the vitamin-A sample is stronger at high-pressure conditions. Taking the commonly known idea into account that fragile liquids are structurally less stable than strong liquids, we can assume that amorphous vitamin-A acetate in the condition of high compression is more stable than at ambient pressure [37,38].

Finally, it is of interest to check whether there are any differences in the shape of the dielectric loss spectra measured at ambient and elevated pressures. In order to analyze the data in a more quantitative way, we have compared two dielectric loss spectra of supercooled retinyl acetate measured at ambient and elevated pressures ( $p = 240$  MPa). The spectra were chosen so that the frequencies of the maximum of the  $\delta$ -relaxation peaks were the same. From the comparison

presented in Fig. 10, it can be easily seen that the high-frequency side of the spectrum becomes slightly broader at an elevated pressure. This effect is mainly due to the increase in the dielectric strength of the  $\alpha$ -relaxation peak. However, the dielectric strength of the  $\delta$ -relaxation process decreases. The drop in amplitude of the  $\delta$ -relaxation peak is probably related to an increase in the molecular packing that hinders reorientations of molecules around the short molecular axis.

#### IV. CONCLUSIONS

The broadband dielectric relaxation measurements of amorphous vitamin-A acetate in the equilibrium liquid state at ambient as well as elevated pressures reveal three relaxation processes:  $\alpha$ ,  $\delta$ , and  $\nu$ . It was found that the  $\delta$ - (Debye-like) process is probably due to the rotational fluctuations of the retinyl molecule around the short axis. It is worth noting that the occurrence of this movement may imply the existence of nanoscale domains with nematic order. This proposed self-organization of molecules is possible because the vitamin-A acetate particle has a rodlike shape, and it is strongly anisotropic. The next  $\alpha$  peak, visible at the high-frequency flank of the dielectric spectra, is probably due to the cooperative motions of the retinyl acetate molecules. Thus, the  $\alpha$ -relaxation process was considered to be responsible for the relaxation of the molecular structure and the liquid-glass transition. The glass transition temperature  $T_g$  and fragility index  $m_P$  of vitamin-A acetate have been determined at ambient and elevated pressures. It is found that the value of  $m_P$  decreases with pressure, and the rate of increase of  $T_g$  with pressure is comparable to other van der Waals glass formers. That is why one can classify the examined retinyl as van der Waals material. The dielectric measurements carried out in the glassy state show two secondary modes:  $\beta$  and  $\gamma$ . The low value of activation energy, obtained for the  $\gamma$  relaxation (23 kJ/mol), which is in good agreement with the value estimated on the basis of the computational simulations, implies that the intramolecular motions are responsible for the occurrence of this mode in the dielectric spectrum.

#### ACKNOWLEDGMENTS

The authors Z.W., M.P., and P.W. are profoundly thankful for the financial support of their research within the framework of the project entitled From Study of Molecular Dynamics in Amorphous Medicines at Ambient and Elevated Pressure to Novel Applications in Pharmacy (Contract No. TEAM/2008–1/6), which is operated within the Foundation for the Polish Science Team Programme cofinanced by the EU European Regional Development Fund.

- [1] K. Albert, G. Schlotterbeck, U. Braumann, H. Handel, M. Spraul, and G. Krack, *Angew. Chem.* **34**, 1014 (1995).  
 [2] K. Grzybowska, M. Paluch, A. Grzybowski, Z. Wojnarowska, L. Hawelek, K. Kolodziejczyk, and K. Ngai, *J. Phys. Chem. B* **114**, 12792 (2010).

- [3] K. Adrjanowicz, K. Kaminski, Z. Wojnarowska, M. Dulski, L. Hawelek, S. Pawlus, and M. Paluch, *J. Phys. Chem. B* **114**, 6579 (2010).  
 [4] L. Gunawan, G. P. Johari, and R. M. Shanker, *Pharm. Res.* **23**, 967 (2006).

- [5] G. P. Johari, S. Kim, and R. M. Shanker, *J. Pharm. Sci.* **96**, 1159 (2007).
- [6] K. L. Ngai and M. Paluch, *J. Chem. Phys.* **120**, 857 (2004).
- [7] K. L. Ngai, R. Casalini, S. Capaccioli, M. Paluch, and C. M. Roland, *Adv. Chem. Phys.* **133**, 497 (2006).
- [8] K. L. Ngai and M. Paluch, *J. Chem. Phys.* **120**, 857 (2004).
- [9] K. L. Ngai, *J. Phys. Condens. Matter.* **15**, S1107 (2003).
- [10] B. C. Hancock and M. Parks, *Pharm. Res.* **17**, 397 (2000).
- [11] B. C. Hancock and G. Zografi, *J. Pharm. Sci.* **86**, 1 (1997).
- [12] K. Kaminski, E. Kaminska, K. Adrjanowicz, K. Grzybowska, P. Włodarczyk, M. Paluch, A. Burian, J. Ziolo, P. Lepek, J. Mazgalski, and W. Sawicki, *J. Pharm. Sci.* **99**, 94 (2009).
- [13] S. L. Shamblin, X. Tang, L. Chang, B. C. Hancock, and M. Pikal, *J. Phys. Chem. B* **103**, 4113 (1999).
- [14] S. L. Shamblin, B. C. Hancock, Y. Dupuis, and M. J. Pikal, *J. Pharm. Sci.* **89**, 417 (2000).
- [15] M. Letz, R. Schilling, and A. Latz, *Phys. Rev. E* **62**, 5173 (2000).
- [16] M. Malkovsk, C. Dore, R. Hunt, L. Palmer, P. Chandler, and P. Medawar, *Proc. Natl. Acad. Sci. U.S.A.* **80**, 6322 (1983).
- [17] F. Neese, *ORCA, an Ab Initio, Density Functional and Semiempirical Program Package*, Version 2.6 (University of Bonn, Bonn, 2008).
- [18] M. J. Frisch, G. W. Trucks, H. B. Schlegel *et al.*, *GAUSSIAN 03*, Revision C.02 (Gaussian, Inc., Wallingford, CT, 2004).
- [19] S. Havriliak and S. Negami, *Polymer* **8**, 161 (1967).
- [20] M. Mierzwa, M. Paluch, S. J. Rzoska, J. Ziolo, and U. Maschke, in *Soft Matter under Exogenic Impacts*, edited by S. J. Rzoska and V. Mazur (Springer, Berlin, 2007).
- [21] A. R. E. Brás, O. García, M. T. Viciosa, S. Martins, R. Sastre, C. J. Dias, J. L. Figueirinhas, and M. Dionísio, *Liq. Cryst.* **35**, 429 (2008).
- [22] K. Asami, *Prog. Polym. Sci.* **27**, 1617 (2002).
- [23] A. Hacura and B. Kaczorowska, *J. Raman Spectrosc.* **36**, 1029 (2005).
- [24] H. Vogel, *Phys. Z.* **22**, 645 (1921).
- [25] G. Fulcher, *J. Am. Ceram. Soc.* **8**, 339 (1923).
- [26] G. Tammann and W. Hesse, *Z. Anorg. Allg. Chem.* **156**, 245 (1926).
- [27] G. Floudas, M. Paluch, A. Grzybowski, and K. L. Ngai, *Molecular Dynamics of Glass-Forming Systems: Effects of Pressure* (Springer, Berlin, 2011).
- [28] M. Naoki and M. Matsushita, *Bull. Chem. Soc. Jpn.* **56**, 2396 (1983).
- [29] H. Forsman, P. Anderson, and G. Bäckström, *J. Chem. Soc., Faraday Trans.* **2**, 857 (1986).
- [30] S. Glasstone, K. J. Laidler, and H. Eyring, *Theory of Rate Processes* (McGraw-Hill, New York, 1941).
- [31] J. M. O'Reilly, *J. Polym. Sci.* **57**, 429 (1962).
- [32] T. Atake and C. A. Angell, *J. Phys. Chem.* **83**, 3218 (1979).
- [33] R. Böhmer, K. L. Ngai, C. A. Angell, and D. J. Plazek, *J. Chem. Phys.* **99**, 4201 (1993).
- [34] K. Adrjanowicz, K. Kaminski, Z. Wojnarowska, M. Dulski, L. Hawelek, S. Pawlus, and M. Paluch, *J. Phys. Chem. B.* **114**, 6579 (2010).
- [35] Z. Wojnarowska, K. Adrjanowicz, P. Włodarczyk, E. Kaminska, K. Kaminski, K. Grzybowska, R. Wrzalik, M. Paluch, and K. L. Ngai, *J. Phys. Chem. B* **113**, 12536 (2009).
- [36] C. M. Roland, S. Hensel-Bielowka, M. Paluch, and R. Casalini, *Rep. Prog. Phys.* **68**, 1405 (2005).
- [37] C. A. Angell, *J. Non-Cryst. Solids* **13**, 131 (1991).
- [38] R. Richert and C. A. Angell, *J. Chem. Phys.* **108**, 9016 (1998).